Cellular Signalling 53 (2019) 151–161

Contents lists available at ScienceDirect

Cellular Signalling

journal homepage: www.elsevier.com/locate/cellsig

S1PR2 antagonist alleviates oxidative stress-enhanced brain endothelial permeability by attenuating p38 and Erk1/2-dependent cPLA$_2$ phosphorylation

Changchun Cao[a,b], Li Dai[a], Junyu Mu[a], Xiaofei Wang[a], Yali Hong[a], Chao Zhu[a], Lai Jin[a], Shengnan Li[a,*]

[a] Department of Pharmacology, Nanjing Medical University, 101 Longmian Avenue, Nanjing 211116, Jiangsu, China
[b] Jiangsu College of Nursing, 9 Science and Technology Avenue, Huaian, 223005, Jiangsu, China

ARTICLE INFO

Keywords:
Sphingosine-1-phosphate receptor-2
Endothelial permeability
Phosphorylation
Cerebral ischemia
Oxidative stress

ABSTRACT

Both sphingosine-1-phosphate receptor-2 (S1PR2) and cytosolic phospholipase A$_2$ (cPLA$_2$) are implicated in the disruption of cerebrovascular integrity in experimental stroke. However, the role of S1PR2 in induction of cPLA$_2$ phosphorylation during cerebral ischemia-induced endothelial dysfunction remains unknown. This study investigated the effect of S1PR2 blockade on oxidative stress-induced cerebrovascular endothelial barrier impairment and explored the possible mechanisms. In bEnd3 cells, cPLA$_2$ inhibitor CAY10502 as well as S1PR2 antagonist JTE013 profoundly suppressed hydrogen peroxide (H_2O_2)-induced changes of paracellular permeability and ZO-1 localization. Besides p38, extracellular signal-regulated kinase (Erk) 1/2 is required for H_2O_2-increased cPLA$_2$ phosphorylation and endothelial permeability. Pharmacological and genetic inhibition of S1PR2 significantly suppressed their phosphorylation in response to H_2O_2. Especially lentivirus-mediated knockdown of S1PR2 inhibited H_2O_2-induced ZO-1 redistribution and paracellular hyperpermeability. Using the permanent middle cerebral artery occlusion (pMCAO) mouse model, we found JTE013 pretreatment markedly reduced Evans blue dye (EBD) extravasation and reversed the decrease in VE-cadherin, occludin, claudin-5 and CD31 expression in infarcted hemisphere. Lentivirus-mediated S1PR2 knockdown also attenuated EBD extravasation. Furthermore, JTE013 pretreatment attenuated neurological deficit, brain edema and infarction volume. Therefore, our findings suggest the protective effect of JTE013 on brain endothelial barrier integrity is likely mediated by suppressing p38 and Erk1/2-dependent cPLA$_2$ phosphorylation under oxidative stress.

1. Introduction

Blood-brain barrier (BBB) impairment is a progressive process involved in ischemic stroke [1,2]. Within the neurovascular unit, the BBB is a highly specialized brain endothelial structure, which is essential for proper brain functions [3,4]. The specialized endothelial cells (ECs) of BBB contain abundant junction proteins, which generate a paracellular seal, allowing efficient transport of select molecules into the central nervous system (CNS) [5–7]. Thus, in the development of cerebral ischemia, EC impairment may contribute to the greatly increased BBB permeability.

The endothelium is responsible for reactive oxygen species (ROS) generation which occurs at the site of the BBB [8]. ROS production increases after permanent and reversible MCAO [9], which mediates oxidative stress and contributes to BBB breakdown [10–12]. H_2O_2, a representative and stable ROS, modulates endothelial permeability [13,14] and impairs the barrier function of cerebrovascular ECs [15,16]. Thus, to mimic in vitro the effect of oxidative stress on cerebrovascular endothelium [12], we exposed the bEnd3 cells to H_2O_2.

S1P, which is identified as a potent biolipid modulator of vascular endothelial integrity, interacts with five specific G-protein-coupled receptors [17]. Among these receptors, S1PR1, S1PR2 and S1PR3 are expressed in various cells including vascular ECs [18,19], whereas the expression of S1PR4 is specifically abundant in immune cells and S1PR5 is mainly expressed in the CNS [20]. Both S1PR1 and S1PR3 are required for S1P-induced junction protein assembly [18], which is needed for enhancement of vascular endothelial barrier function [17]. Strikingly, in the human cerebrovasculature S1PR5 activation enhances EC barrier integrity [21]. On the contrary, activation of S1PR2 enhances vascular permeability through Rho-ROCK (Rho-associated

* Corresponding author.
E-mail address: snli@njmu.edu.cn (S. Li).

https://doi.org/10.1016/j.cellsig.2018.09.019
Received 18 August 2018; Received in revised form 19 September 2018; Accepted 25 September 2018
Available online 02 October 2018
0898-6568/

kinase)-PTEN (phosphatase and tensin homolog deleted on chromosome 10) dependent pathways [19]. More importantly, S1PR2 plays a critical role in the induction of cerebrovascular permeability after ischemia-reperfusion (I/R) injury and matrix metalloproteinases (MMP)-9 activation in brain ECs [22].

It is well established that the phosphorylation of $cPLA_2$ by mitogen-activated protein kinase (MAPK) on Serine-505 increases its catalytic activity [23,24]. $cPLA_2$ is a vital enzyme mediating arachidonic acid (AA) release, which has been implicated in cerebral ischemia-induced oxidative injury and cerebrovascular permeability change [10,11,25,26]. Activation of MAPK, including p38 and Erk1/2, has been reported to be involved in I/R damage after transient MCAO (tMCAO) [10,27] and related to $cPLA_2$ activity [10,11]. In lung epithelial cells, S1P through S1PR3 promoted $cPLA_2$ phosphorylation and AA release via a flux of intracellular free calcium and MAPK and ROCK-dependent pathways [28]. Besides, our previous data showed that S1P release in vascular smooth muscle cells up-regulated $cPLA_2$ expression by activating S1PR3 [29]. Since S1PR3 and S1PR2 have opposite effects on maintenance of endothelial function [18,19,21], we aimed to assess the association of S1PR2 with $cPLA_2$ in oxidative stress-induced endothelial barrier impairment in this study.

Reperfusion strategy is the most effective therapy for stroke and I/R-associated BBB injury has been intensively investigated [30]. Unfortunately, in practice, the effective therapeutic window limits the reperfusion therapy for acute ischemic stroke [31]. Therefore, another important problem to solve is whether S1PR2 blockade remains effective for ischemic injuries when the duration of ischemia is prolonged. And hence we performed the pMCAO model in mice.

Here we report that both S1PR2 and $cPLA_2$ activation mediate tight junction alteration in response to H_2O_2, increasing the bEnd3 cell monolayer permeability. On the other hand, H_2O_2-increased serine-505 phosphorylation of $cPLA_2$ and bEnd3 cell monolayer hyperpermeability depend on the activation of p38 as well as Erk1/2. Moreover, blockade and knockdown of S1PR2 protect endothelial barrier integrity during acute cerebral ischemia in vivo. Therefore, S1PR2 antagonist appears to protect brain ECs against oxidative stress-induced permeability change through inhibiting the p38 and Erk1/2-dependent $cPLA_2$ phosphorylation.

2. Materials and methods

2.1. Animals

Adult male C57BL/6 mice (6–8 weeks, $n = 212$) were purchased from the Model Animal Research Center of Nanjing University (Nanjing, China). In accordance with the guidelines of the Nanjing Medical University's Regulations of Animal Experiments, mice were raised in a pathogen-free barrier facility with a regulated 12-h light/dark cycle with water and food ad libitum for 7 days before experiment to adapt to the circumstances. All experiments were approved by the Animal Experiment Committee of the Nanjing Medical University.

2.2. Cell cultures and chemicals

Mouse brain microvascular ECs bEnd3 (American Type Culture Collection), passage 25–35, were grown as a monolayer in Dulbecco's modified Eagle's medium supplemented with 10% fetal bovine serum at 37 °C in a humidified atmosphere of 5% CO_2 and 95% air, as described previously [22,32,33].

JTE013 was purchased from Santa Cruz Biotechnology. U0126, SB203580 and FR180204 were obtained from Selleck. CAY10502 was from Cayman.

2.3. Transendothelial permeability assay

Transendothelial permeability was measured as previously described [14]. Briefly, bEnd3 cells (1×10 [5]) were seeded on 24-well hanging inserts (0.4 μm pore size, Millipore Millicell) in 24-well dishes and cultured for 12 h. Then cells were serum-starved for 4 h and treated with vehicle (DSMO) or indicated chemicals for 2 h prior H_2O_2 (2 mM) stimulation for 1 h. Immediately after H_2O_2 addition 5 μL of FITC-dextran (molecular weight 40,000, Sigma-Aldrich, final concentration 1 mg/mL) was added to the inserts. The inserts were taken out and samples were taken from the lower dishes after H_2O_2 treatment. The fluorescence intensity of FITC-dextran in the samples was measured in duplicate per condition at 492/520 nm excitation /emission wavelengths.

2.4. Lentiviral constructs and short hairpin RNA (shRNA) for S1PR2

S1PR2 shRNA (shS1PR2) and negative control shRNA (shNC) lentivirus vectors with a red fluorescent protein (RFP) tag were obtained from Genepharma (Shanghai, China). To generate the shS1PR2, a target sequence was designed against mouse S1PR2: GCCATCGTGGTGGAGA ATCTT. According to the manufacturer's instructions, bEnd3 cells were incubated with lentivirus for 24 h and then the medium was changed. After incubation for an additional 72 h, the knockdown efficiency at the protein level was assessed by western blot analysis.

2.5. Immunofluorescence staining

Immunostaining procedure was performed as previously reported [16]. The confluent cells were incubated with anti-ZO-1 (21773–1-AP) (1:100, Proteintech) primary antibody at 4 °C overnight, followed by incubation with the Alexa Fluor 488 (SA00006–2) or Alexa Fluor 594 (SA00006–4) -conjugated secondary antibody (1:100, Proteintech). DAPI (KeyGEN BioTECH, Nanjing, China) was used to stain nuclei.

2.6. Animal surgery and drug administration

The pMCAO was performed following previously described methods with minor modification [34]. Briefly, surgery was performed by a dissecting surgical microscope. Body temperature was maintained constant (37 ± 0.5 °C) with a heating pad and lamp. Under chloral hydrate anesthesia (300 mg/kg, i.p.), a nylon monofilament (6–0) with with a round tip was gently inserted from the right external carotid artery stump to the internal carotid artery and stopped at the origin of the MCA. The distance from the bifurcation of internal/external carotid artery to MCA was 10 ± 0.5 mm. Successful occlusion was verified by monitoring regional cerebral blood flow with laser Doppler flowmetry. In the sham-operated mice, the nylon monofilament was inserted along the internal carotid artery and then immediately withdrawn.

Animals were randomly assigned to the treatment groups. Vehicle or JTE013 (30 mg/kg) [22] was injected intraperitoneally 30 min before the onset of pMCAO.

2.7. Neurological score assessment

Neurological scoring was performed by an independent investigator blinded to the experimental groups at 24 h after MCAO according to a 5-point scale as previously described [34].

2.8. Measurement of infarct volume and brain edema

After assessment of neurological scores, cerebral infarct volumes were measured as described previously [35]. Mice were euthanized and brains were harvested rapidly. Seven coronal sections of the brain (1 mm thickness) were incubated in 2% 2,3,5-triphenyltetrazolium chloride (TTC, Sigma-Aldrich) for 30 min at 37 °C. Scanned images were used to calculate infarct and edema ratios by image analysis software (Image J, NIH). Difference between contralateral and ipsilateral hemisphere volumes indicates brain edema development, and therefore infarct ratios were calculated after normalization by the

contralateral hemisphere and corrected for edema as reported previously [22].

2.9. EBD extravasation assay

At 12 h after MCAO, 2% EBD (Sigma-Aldrich) solution (4 mL/kg) in normal saline was administered intravenously. The animals were anesthetized 2 h later and perfused through the left ventricle with ice-cold normal saline to remove intravascular dye. Brains were harvested, sliced and scanned. The hemispheres were weighted and homogenized in 50% trichloroacetic acid solution, then centrifuged at 20000*g* for 20 min. Then the supernatant was diluted 4-fold with ethanol. The extravascular EBD amount was calculated by measuring the fluorescence intensity (620/680 nm excitation/emission) of the supernatant.

2.10. Stereotactic injection

For all surgical procedures, mice were anesthetized. We carried out the cortical injection of shNC or shS1PR2 lentivirus using a stereotaxic instrument (RWD Life Science, Shenzhen, China) as previously described with minor modification [35,36]. Each mouse was subjected to three cortical injections in the right hemisphere (i.e., ipsilateral to the MCAO) at the following coordinates: point 1, 1.5 mm anterior to the bregma, 2.5 mm lateral, 2 mm deep; point 2, 0.5 mm posterior to the bregma, 3 mm lateral, 2 mm deep; point 3, 2 mm posterior to the bregma, 3 mm lateral, 2 mm deep. 1 μL of lentivirus suspension containing 1 × 10 [9] TU/mL was injected in each point at a rate of 0.2 μL/min. The needle was withdrawn over a course of 15 min. Seven days after injection of lentivirus, mice were perfused for histology or subjected to pMCAO as described above.

2.11. Histology

As previously described [36], mice were anesthetized and perfused transcardially. The brains were post-fixed in 4% paraformaldehyde (PFA) for 24 h and then transferred to a 30% sucrose solution in phosphate buffer solution (PBS) for 2 days. 20 μm thick coronal sections sliced on a freezing microtome (Leica CM1950) were incubated with DAPI for 10 min to label cell nuclei. Endogenous viral expression of fluorophores was imaged on a fluorescence microscope (OLYMPUS IX70).

2.12. Western blot analysis

Protein extracts from brain tissues and cultured cells were prepared and analyzed by western blot as reported previously [11,29]. Primary antibodies were anti-phospho-p38 (Thr180/Tyr182) (#4511), anti-p38 (#8690), anti-phospho-cPLA$_2$ (Ser505) (#2831), anti-CD31 (#77699) (all 1:1000, Cell Signaling Technology), anti-cPLA$_2$ (sc-454), anti-phospho-Erk1/2 (Thr202/Tyr204) (sc-136,521), anti-Erk1/2 (sc-514,302), anti-EDG5 (S1PR2) (sc-365,963) (all 1:500, Santa Cruz Biotechnology), anti-Occludin (13409–1-AP), anti-PSD95 (20665–1-AP) and anti-ZO-1 (21773–1-AP) (all 1:1000, Proteintech), anti-Claudin-5 (ab15106) and anti-VE-cadherin (ab205336) (1:1000, Abcam). Appropriate horseradish peroxidase-linked secondary antibodies (1:10000, Proteintech) were used for detection by enhanced chemiluminescence (Bio-Rad). To control sample loading and protein transfer, the PVDF membranes (Roche) were stripped and reprobed with Tubulin-beta antibody (10094–1-AP) (1:5000, Proteintech).

2.13. Statistical analysis

All values reported are mean ± SEM. For comparison between 2 groups, Statistical differences were evaluated by the unpaired Student *t*-test. For comparison among multiple groups, statistical differences were calculated by one-way ANOVA followed by Newman-Keuls test. The neurological scores were analyzed with a nonparametric test (Mann-Whitney *U* test). The criterion for statistical significance was set at $P < 0.05$.

3. Results

3.1. S1PR2 antagonist and cPLA$_2$ inhibitor suppress H_2O_2-induced monolayer hyperpermeability and tight junction alteration in bEnd3 cells

To assess the effect of S1PR2 antagonist on H_2O_2-induced brain endothelial permeability change, the penetration of high molecular weight FITC-dextran across bEnd3 cell monolayer was measured by the transwell assay. H_2O_2 stimulation led to a significant increase in paracellular permeability. And the pretreatment of S1PR2 antagonist JTE013 markedly decreased H_2O_2-induced endothelial hyperpermeability without altering basal permeability (Fig. 1A). Interestingly, pretreatment with the cPLA$_2$ inhibitor CAY10502 also attenuated H_2O_2-induced endothelial hyperpermeability (Fig. 1B).

To further examine the effect of JTE013 and CAY10502 on endothelial tight junction integrity, the localization of ZO-1 was examined by immunofluorescence staining in the absence or presence of H_2O_2. As shown in Fig. 1C and D, control ZO-1 had a continuous distribution at cell junctions. H_2O_2 changed this distribution pattern to a more discontinuous one with loss of junctional localization, which was suppressed by the pretreatment of CAY10502 as well as JTE013. However, neither JTE013 nor CAY10502 affected the localization of ZO-1 alone.

3.2. Activation of p38 as well as Erk1/2 is required for H_2O_2-induced cPLA$_2$ phosphorylation in bEnd3 cells

To elucidate the relationship between MAPK activation and cPLA$_2$ phosphorylation under oxidative stress, we stimulated bEnd3 cells with H_2O_2 and analyzed the protein phosphorylation by western blot analysis. As shown in Fig. 2A, H_2O_2 treatment induced a sustained high level of p38 phosphorylation. Erk1/2 phosphorylation increased within 5 min after H_2O_2 treatment which caused continuous activation of Erk1/2 phosphorylation up to 60 min. And the maximal increase of Erk1/2 activation was detected at 15 min. Similar to Erk1/2, cPLA$_2$ phosphorylation after H_2O_2 treatment also increased at 5 min, achieved the maximum at 15 min, and was maintained for 60 min.

Then we addressed whether Erk1/2 activation could directly contribute to the regulation of cPLA$_2$ phosphorylation after H_2O_2 treatment. As shown in Fig. 2B, pretreatment with the specific MAPK/Erk kinase (MEK) 1/2 inhibitor U0126 simultaneously suppressed H_2O_2-induced increase in Erk1/2 and cPLA$_2$ phosphorylation dose-dependently. The selective Erk inhibitor FR180204 also inhibited H_2O_2-induced concomitant increase in Erk1/2 and cPLA$_2$ phosphorylation in a dose-dependent fashion (Fig. 2C). At the same time, U0126 as well as FR180204 did not significantly inhibit the phosphorylation of p38 (Fig. 2B and C).

Given that p38 is a kinase upstream of cPLA$_2$, we next evaluated the impact of p38 activation on H_2O_2-induced Erk1/2 and cPLA$_2$ phosphorylation. The pretreatment of SB203580, a selective p38 inhibitor, substantially decreased the phosphorylation of p38 and cPLA$_2$ but not Erk1/2 after H_2O_2 treatment (Fig. 2D). Moreover, pretreatment with CAY10502 remarkably inhibited H_2O_2-induced increase in cPLA$_2$ phosphorylation (Fig. 2D).

3.3. S1PR2 regulates H_2O_2-enhanced cPLA$_2$ phosphorylation by inducing p38 and Erk1/2 activation in bEnd3 cells

To investigate whether S1PR2 antagonist could inhibit oxidative stress-induced cPLA$_2$ phosphorylation, we pretreated bEnd3 cells with JTE013 before H_2O_2 exposure. As shown in Fig. 3A-D, incubation with H_2O_2 resulted in the phosphorylation of p38, Erk1/2 and cPLA$_2$ in a dose-dependent manner, which was significantly suppressed by JTE013 pretreatment. Moreover, neither H_2O_2 nor JTE013 changed the protein

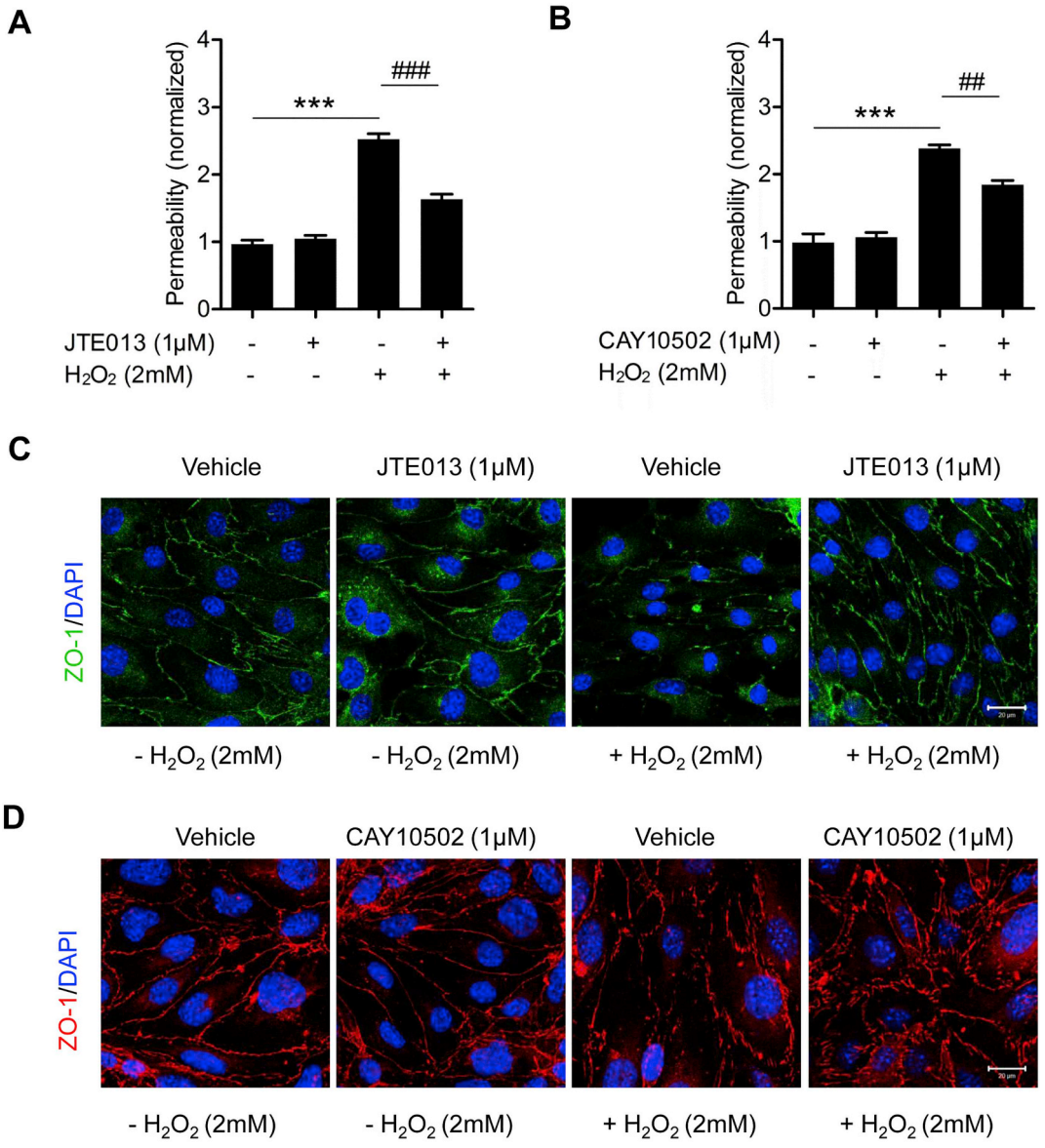

Fig. 1. S1PR2 antagonist and cPLA$_2$ inhibitor suppress H_2O_2-induced endothelial hyperpermeability and ZO-1 redistribution in vitro. (A and B) Endothelial permeability was measured by the FITC-dextran assay. Fluorescence intensity was normalized to vehicle-treated cells. (C and D) Confocal images of ZO-1-immunolabeled (C, green. D, red) and DAPI-stained (blue) bEnd3 cells. After 4 h of serum starvation, cells were treated with vehicle, 1 μM JTE013 (A and C) or 1 μM CAY10502 (B and D) for 2 h before 2 mM H_2O_2 stimulation for 1 h. Scale bar, 20 μm. Data are presented as mean ± SEM, n = 4/group. $^{***}P < 0.001$ versus vehicle; $^{\#\#}P < 0.01$, $^{\#\#\#}P < 0.001$ versus vehicle + H_2O_2. (For interpretation of the references to colour in this figure legend, the reader is referred to the web version of this article.)

levels of ZO-1, CD31, VE-cadherin and occludin. Next, we confirmed the role of S1PR2 in regulating cerebroendothelial permeability. The pretreatment of FR180204 as well as JTE013 substantially attenuated H_2O_2-induced bEnd3 cell monolayer hyperpermeability, which is consistent with the mild effect of SB203580 and CAY10502 (Fig. 3E).

Using shS1PR2 lentivirus, we effectively knocked down S1PR2 protein expression (~80% reduction) in bEnd3 cells (Fig. 4A-C). After H_2O_2 stimulation, the phosphorylation levels of p38, Erk1/2 and cPLA$_2$ were remarkably decreased in shS1PR2-infected cells (Fig. 4D-G).

3.4. S1PR2 knockdown suppresses H_2O_2-induced tight junction alteration and monolayer hyperpermeability in bEnd3 cells

We next examined the localization of ZO-1 in the absence or presence of H_2O_2, to investigate the effect of S1PR2 knockdown on endothelial tight junction integrity. As shown in Fig. 5A, both shNC-infected and shS1PR2-infected cells exhibited a continuous distribution of ZO-1 at cell junctions. H_2O_2 stimulation led to a discontinuous ZO-1 staining and pronounced disruption of cell junctions in shNC-infected cells, which was inhibited by shS1PR2 treatment. Then we assessed the critical role of S1PR2 in mediating H_2O_2-induced brain transendothelial permeability change. H_2O_2 stimulation resulted in a significant increase in paracellular permeability in shNC-infected cells, while shS1PR2 treatment markedly decreased H_2O_2-induced endothelial hyperpermeability without affecting basal permeability (Fig. 5B).

3.5. S1PR2 antagonist protects the interendothelial junctions from disruption following ischemic stroke

To determine the in vivo effect of JTE013 on BBB disruption after

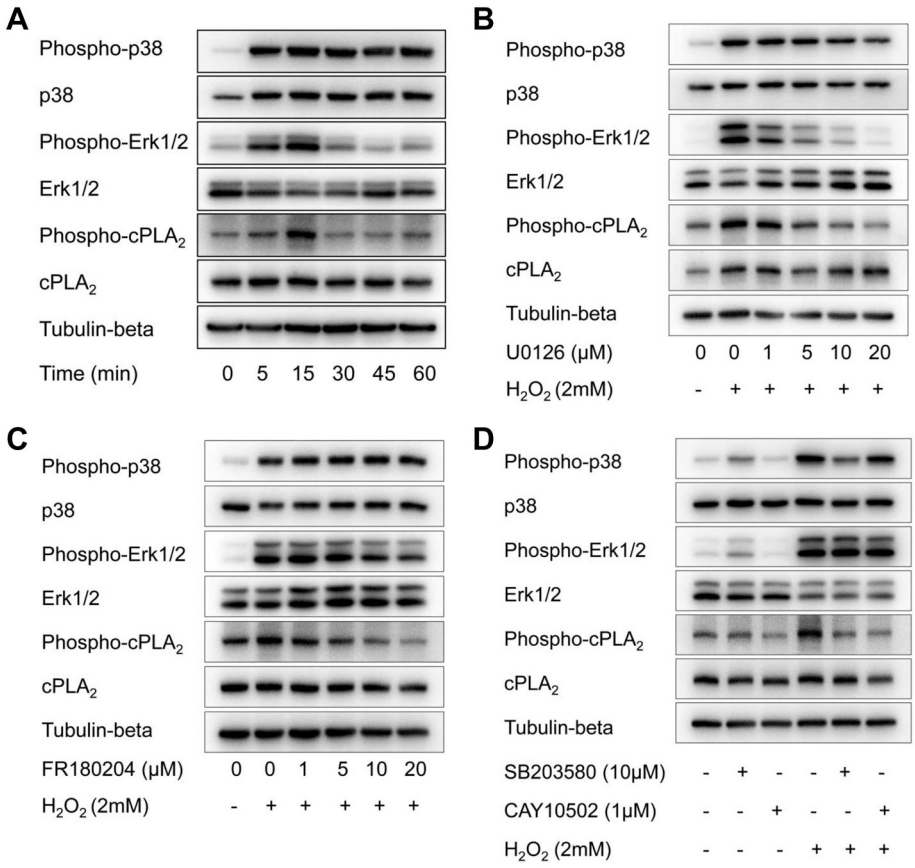

Fig. 2. Activation of p38 as well as Erk1/2 is necessary for H_2O_2-induced $cPLA_2$ phosphorylation. (A) H_2O_2 stimulates phosphorylation of p38, Erk1/2 and $cPLA_2$. The lysates of confluent bEnd3 cells treated with H_2O_2 (2 mM) for the indicated time periods were immunoblotted with antibodies indicated. (B and C) Activation of Erk1/2 is required for H_2O_2-induced $cPLA_2$ phosphorylation. Representative immunoblots show constitutive and concomitant phosphorylated protein in lysates of bEnd3 cells pretreated with U0126 (B) or FR180204 (C) for 2 h at the concentrations indicated and then treated with H_2O_2 (2 mM) for 30 min. (D) Activation of p38 is required for H_2O_2-induced $cPLA_2$ phosphorylation. The bEnd3 cells were treated with vehicle, 10 μM SB203580 or 1 μM CAY10502 for 2 h before 2 mM H_2O_2 stimulation for 30 min. Representative images from 4 independent experiments are shown.

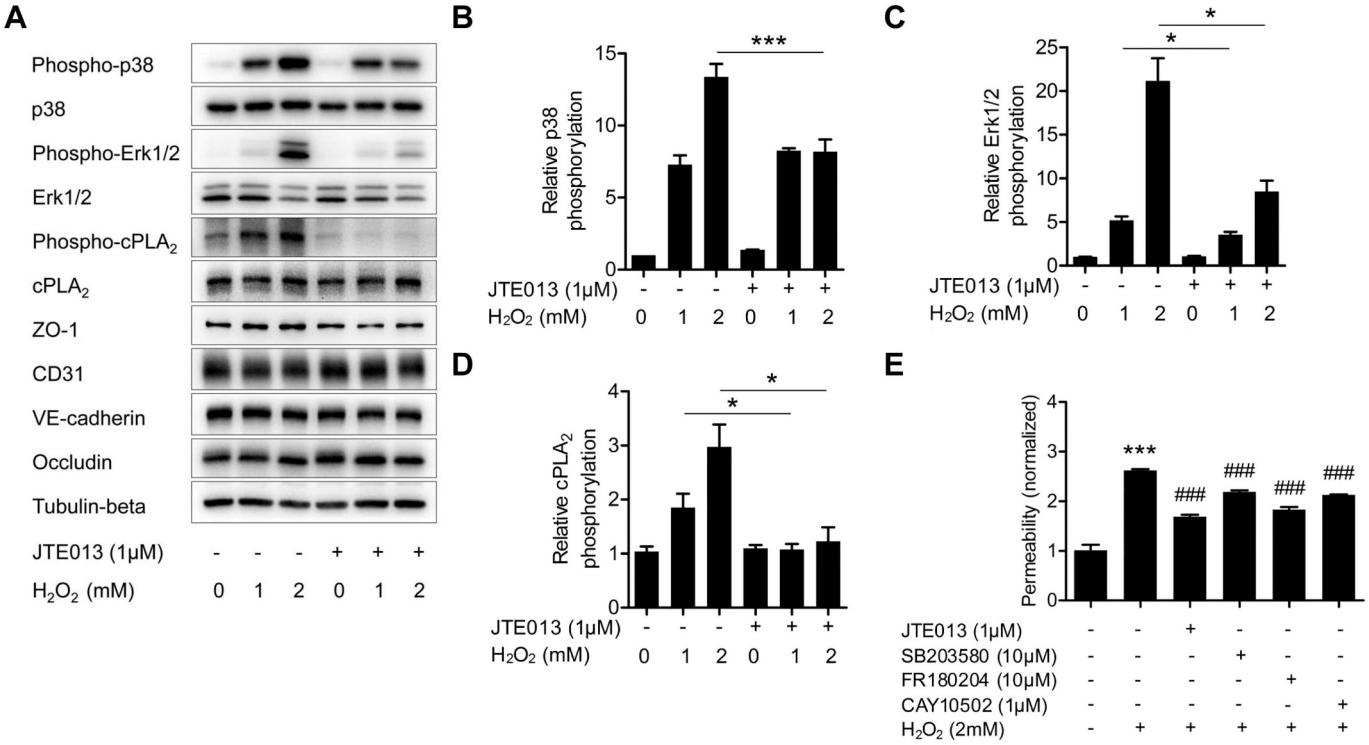

Fig. 3. S1PR2 antagonist JTE013 inhibits H_2O_2-enhanced $cPLA_2$ phosphorylation by attenuating p38 and Erk1/2 activation in bEnd3 cells. (A) The lysates of confluent bEnd3 cells pretreated with JTE013 (1 μM) for 2 h and then exposed to H_2O_2 at the concentrations indicated for 30 min were immunoblotted with antibodies indicated. (B-D) Quantification of p38, Erk1/2 and $cPLA_2$ phosphorylation in (A). Data are obtained from at least 3 independent experiments and represented as mean ± SEM. $^{*}P < 0.05$, $^{***}P < 0.001$ versus vehicle. (E) Blockade of S1PR2 and inhibition of p38, Erk1/2 and $cPLA_2$ reduce H_2O_2-enhanced endothelial permeability in vitro. After 4 h of serum starvation, cells were treated with vehicle, 1 μM JTE013, 10 μM SB203580, 10 μM FR180204 and 1 μM CAY10502 for 2 h before 2 mM H_2O_2 stimulation for 1 h. Endothelial permeability was measured by the FITC-dextran assay. Fluorescence intensity was normalized to vehicle-treated cells. Data are mean ± SEM, n = 4/group. $^{***}P < 0.001$ versus vehicle; $^{\#\#\#}P < 0.001$ versus vehicle + H_2O_2.

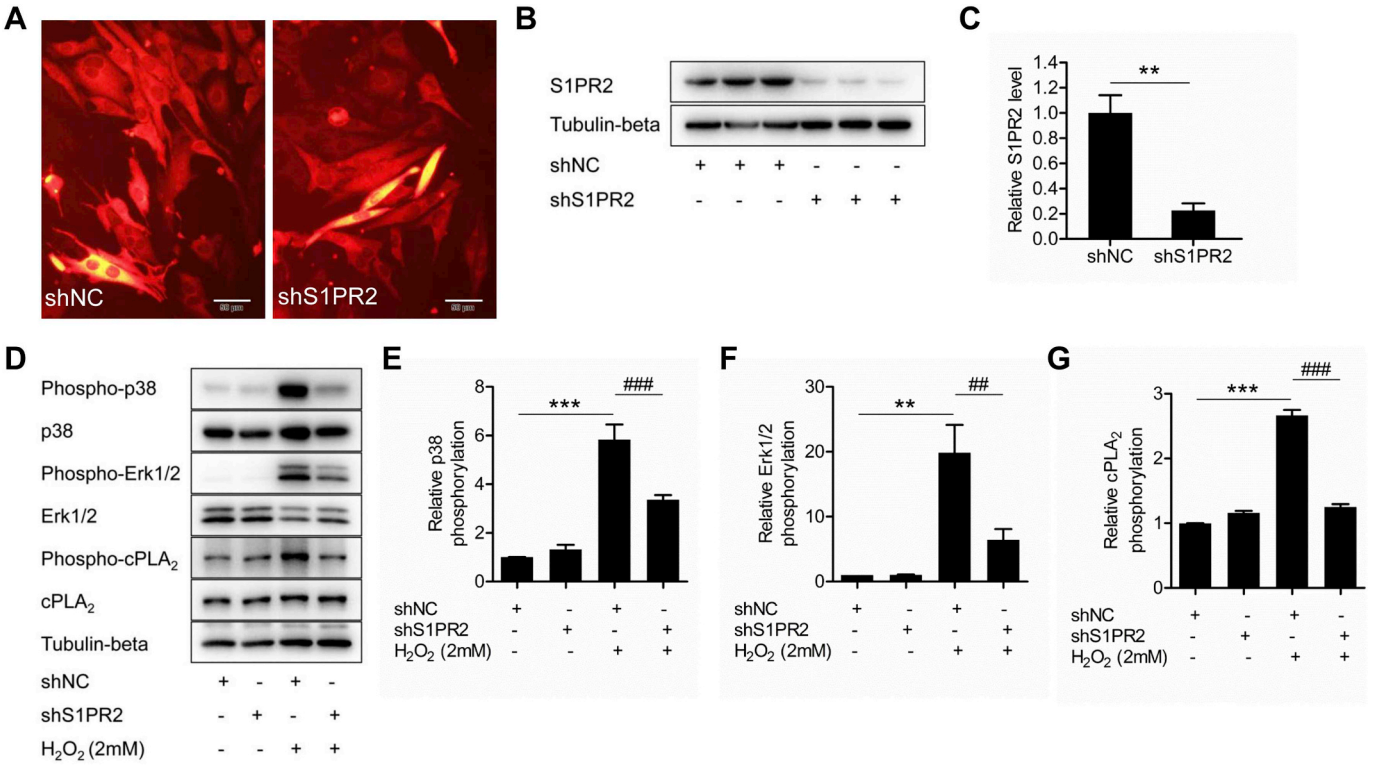

Fig. 4. S1PR2 knockdown inhibits H_2O_2-enhanced $cPLA_2$ phosphorylation by attenuating p38 and Erk1/2 activation in bEnd3 cells. (A) RFP-positive cells indicate the successful infection of shS1PR2 lentivirus. (B) S1PR2 expression was detected by western blot analysis after 96 h of infection. (C) Quantification of S1PR2 in (B). (D) The lysates of lentivirus-infected bEnd3 cells exposed to H_2O_2 (2 mM) for 30 min were immunoblotted with antibodies indicated. (E-G) Quantification of p38, Erk1/2 and $cPLA_2$ phosphorylation in (D). Scale bar, 50 μm. Data are obtained from at least 3 independent experiments and represented as mean ± SEM. $^{**}P < 0.01$, $^{***}P < 0.001$ versus shNC. $^{\#\#}P < 0.01$, $^{\#\#\#}P < 0.001$ versus shNC + H_2O_2.

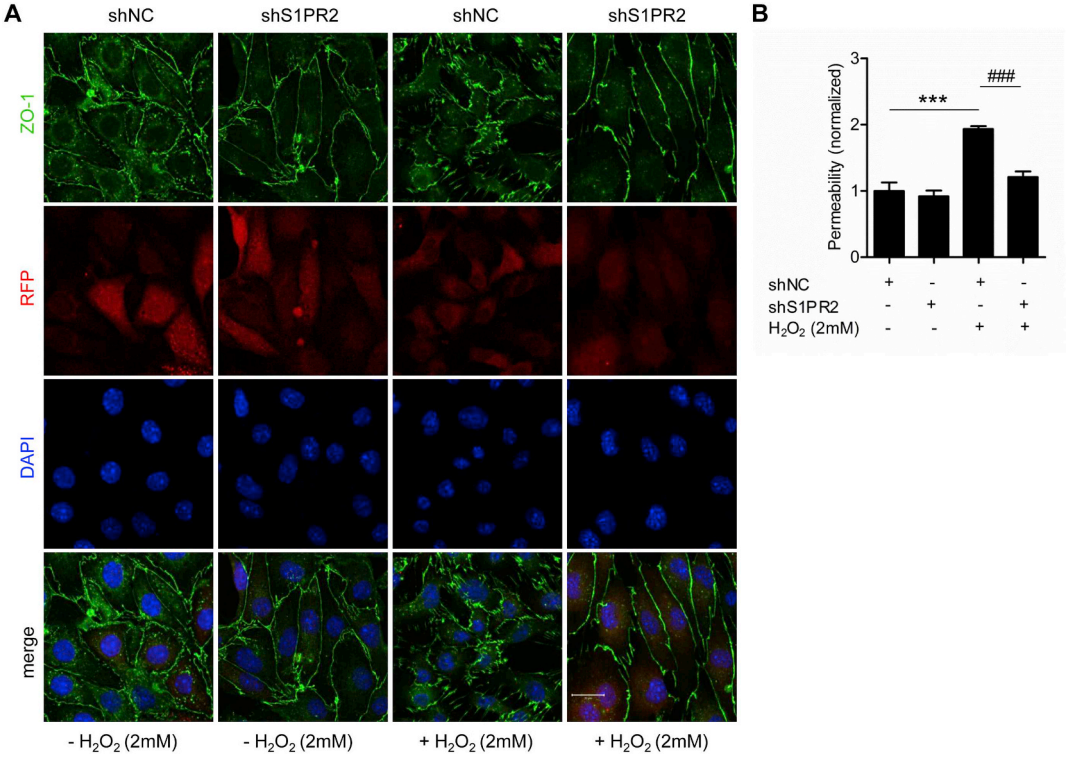

Fig. 5. S1PR2 knockdown suppresses H_2O_2-induced ZO-1 redistribution and brain endothelial hyperpermeability in vitro. (A) Confocal images of ZO-1-immunolabeled (green) and DAPI-stained (blue) bEnd3 cells. (B) Endothelial permeability was measured by the FITC-dextran assay. After 96 h of infection, the lentivirus-infected bEnd3 cells were serum-starved for 4 h and then exposed to H_2O_2 (2 mM) for 1 h. The fluorescence intensity was normalized to vehicle-treated shNC-infected cells. Scale bar, 20 μm. Data are presented as mean ± SEM, n = 4/group. $^{***}P < 0.001$ versus shNC + vehicle; $^{\#\#\#}P < 0.001$ versus shNC + H_2O_2. (For interpretation of the references to colour in this figure legend, the reader is referred to the web version of this article.)

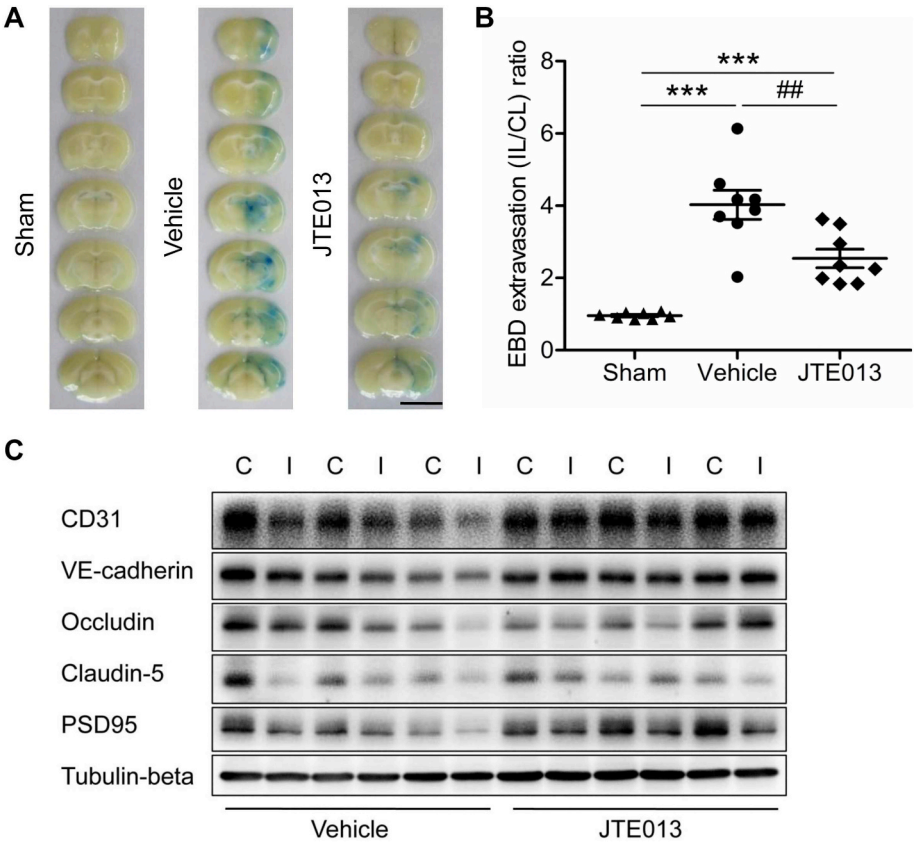

Fig. 6. S1PR2 antagonist JTE013 protects the inter-endothelial junctions from disruption in cerebral ischemia. (A) Brain coronal slices of representative animals. Blue area showed extravasated EBD. (B) Quantification of extravascular EBD (n = 8/group). Ipsilateral/contralateral (IL/CL) ratios are plotted. Scale bar, 5 mm. Data are mean ± SEM. $^{***}P < 0.001$ versus sham; $^{\#\#}P < 0.01$ versus vehicle. (C) Western blot analysis from vehicle or JTE013-treated mice after 12 h of MCAO. Representative images of the indicated protein are shown (n = 3/group). I indicates ipsilateral hemisphere; C, contralateral hemisphere. (For interpretation of the references to colour in this figure legend, the reader is referred to the web version of this article.)

ischemic injury, we used the pMCAO mouse model and measured BBB leakage using EBD extravasation assay (Fig. 6A). After 12 h of MCAO, EBD extravasation ratio was significantly increased in vehicle-treated mouse brain compared with the sham group, and JTE013-treated mice exhibited a dramatic decrease in EBD extravasation ratio (Fig. 6B). To further examine the effect of JTE013 on cerebral vascular EC junction disruption, we detected the total protein levels in the ischemic brain by western blot analysis. As shown in Fig. 6C and Supplementary Fig. 1A-D, the significant increase in protein levels of claudin-5, occludin, VE-cadherin and CD31 was observed in ipsilateral hemispheres of JTE013-treated mice compared with vehicle-treated mice at 12 h after the onset of pMCAO. Nonetheless, JTE013 treatment did not reverse the significant decrease in the synaptic protein PSD95 level in the ipsilateral hemispheres (Supplementary Fig. 1E).

3.6. S1PR2 knockdown prevents the BBB disruption following ischemic stroke

We next tested whether S1PR2 was directly responsible for the BBB damage after cerebral ischemia. Mice were unilaterally injected in the cortex with either shNC or shS1PR2 lentivirus. Seven days later, we observed bright RFP expression at the injection sites (Fig. 7A) and found that shS1PR2 lentivirus effectively reduced the S1PR2 expression in the cortex of mice (Fig. 7B and C). Then we induced ischemia in the right hemisphere by pMCAO and measured EBD extravasation (Fig. 7D). As compared with shNC lentivirus, the treatment of shS1PR2 lentivirus significantly suppressed EBD extravasation in the ipsilateral hemispheres after 12 h of MCAO (Fig. 7E).

3.7. S1PR2 antagonist decreases brain edema, infarction volume and neurological deficit in ischemic stroke

To evaluate the in vivo effect of JTE013 on cerebral ischemic injury, we subjected mice to pMCAO and conducted TTC staining (Fig. 8A). As compared with the control mice, a dramatic decrease in both total cerebral edema ratio (Fig. 8B) and infarct ratio (Fig. 8C), was observed at 24 h after the onset of pMCAO in the JTE013-treated mice. In addition, ischemia-induced neurological deficits were also decreased in JTE013-treated mice at 24 h after MCAO (Fig. 8D).

4. Discussion

The normal BBB protects the neuronal cells efficiently from many harmful substances, while BBB breakdown, a common hallmark of ischemic damage, is associated with elevated cerebrovascular endothelial permeability [4]. ROS produced by the ECs of BBB can mediate oxidative stress, influencing endothelial barrier function, but the pathways involved are incompletely understood. On the other hand, a detailed understanding of the endothelial barrier dysfunction in ischemic injury is important to develop novel therapeutic approaches for cerebrovascular protection. In this study, we have identified a role for S1PR2 in a signaling cascade leading to enhanced endothelial permeability triggered by H_2O_2, a cell-permeant ROS. To summarize our major findings, we could show that: [1] In bEnd3 cells, both S1PR2 and $cPLA_2$ activation mediate tight junction alteration and monolayer permeability increase in response to H_2O_2. [2] The activation of p38 as well as Erk1/2 regulates H_2O_2-induced phosphorylation of $cPLA_2$ and hyperpermeability in vitro. [3] S1PR2 in vivo mediates brain endothelial barrier impairment during acute ischemia.

S1PR2 has a crucial role in regulating vascular endothelial permeability. Its activation in ECs induced disruption of AJs and enhanced paracellular permeability, whereas JTE013 treatment attenuated H_2O_2-evoked rat lung edema [19]. Specifically in the mouse tMCAO, S1PR2 which is up-regulated in cerebral microvessels in the ipsilateral hemispheres activates the MMP-9, exacerbating BBB disruption and neurovascular injury [37], whereas blockade or knockout of S1PR2 improved the cerebrovascular integrity after I/R injury [22], indicating that cerebral ischemia could activate S1PR2 in the cerebrovascular

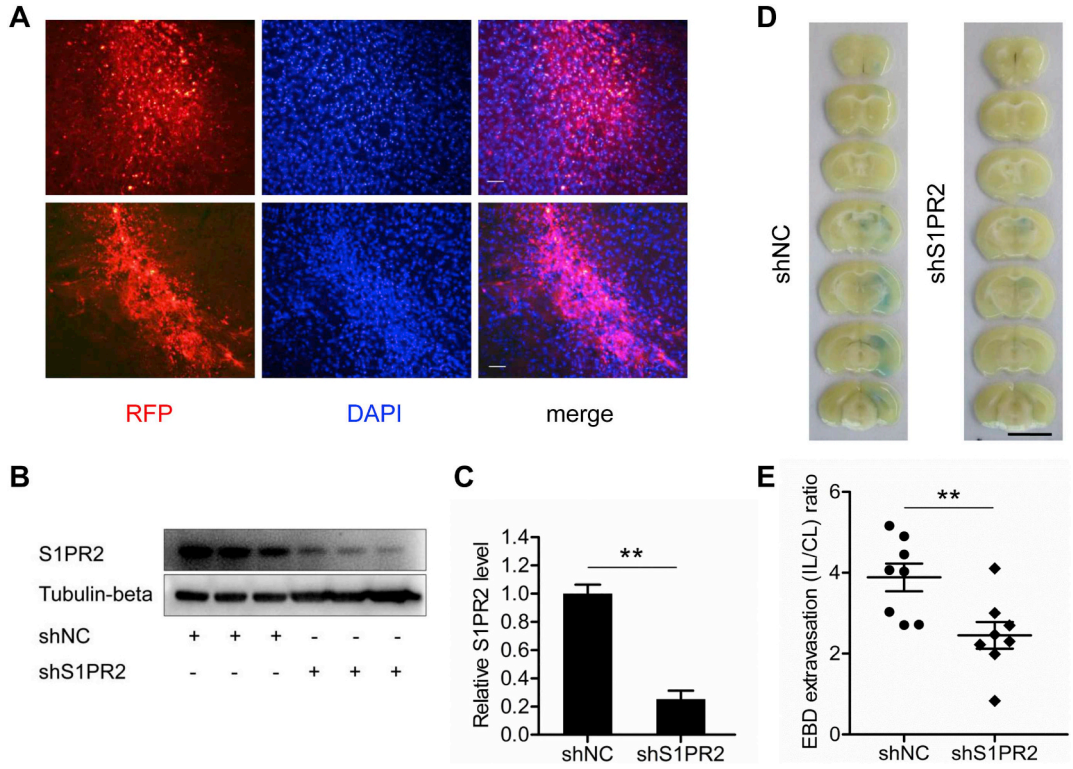

Fig. 7. S1PR2 knockdown prevents BBB breakdown during stroke. (A) The representative fluorescence images of the cortices infected with shS1PR2 lentivirus vectors expressed RFP (red) and stained with DAPI (blue). Scale bar, 50 μm. (B) S1PR2 expression in the cortex of mice was detected by western blot analysis after 7 days of infection. Representative images of the indicated protein are shown (n = 3/group). (C) Quantification of S1PR2 in (B). (D) Brain coronal slices of representative animals. Blue area showed extravasated EBD. (E) Quantification of extravascular EBD (n = 8/group). Ipsilateral/contralateral (IL/CL) ratios are plotted. Scale bar, 5 mm. Data are mean ± SEM.**P < 0.01 versus shNC. (For interpretation of the references to colour in this figure legend, the reader is referred to the web version of this article.)

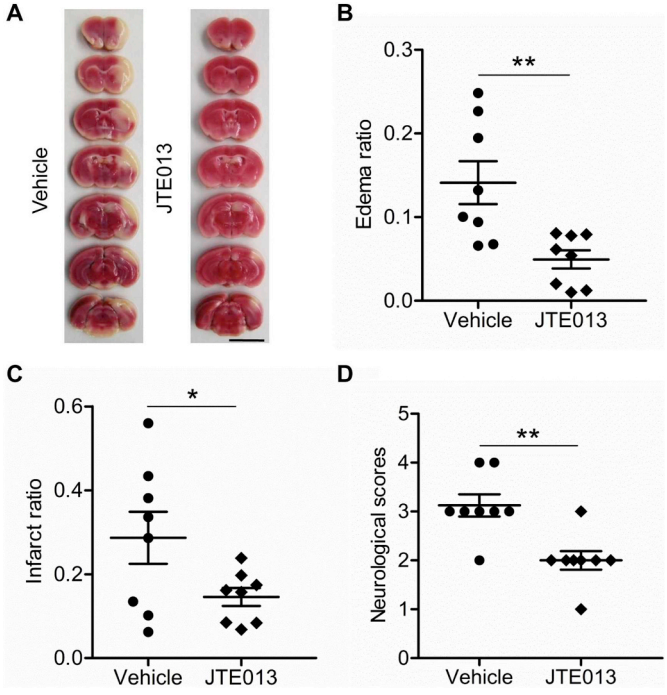

Fig. 8. S1PR2 antagonist JTE013 protects against pMCAO-induced cerebral edema, neuronal injury and neurological deficits. (A) Representative images of TTC staining of seven, 1-mm-thick brain coronal slices 24 h after MCAO. Edema (B) and infarct (C) ratios were calculated by image analysis and reported as a ratio of the contralateral hemisphere. (D) Neurological scores were measured at 24 h after MCAO. Scale bar, 5 mm. Data are mean ± SEM, n = 8/group. *P < 0.05, **P < 0.01 versus vehicle.

endothelium. Under oxidative stress, in contrast to the elusive role of S1PR2 in regulating cerebrovascular endothelial permeability, the activated cPLA$_2$ contributes to ROS generation in permeability responses. After focal I/R, the p38 inhibition in the brain decreased cPLA$_2$ phosphorylation and EBD leakage, evidencing that endothelial AA formation increased ROS formation and stroke-induced cerebrovascular permeability [10]. And cPLA$_2$ modulates the early ischemic cerebral injury after tMCAO via phosphorylation of p38 and Erk1/2 [11]. Furthermore, cPLA$_2$ inhibition [26] and knockout [11,25] reduced transient focal ischemic brain damage in mice. Nevertheless, little is known about the precise relationship between S1PR2 and cPLA$_2$ activation.

Notably, MAPKs, p38 and Erk1/2, activation in the A549 human lung epithelial cell line, partially mediated extracellular S1P-induced cPLA$_2$ phosphorylation and AA release [28]. Thus, we proposed a mechanism in which S1PR2, via MAPK-dependent cPLA$_2$ activation, regulates cerebrovascular endothelial barrier integrity under oxidative stress, thus promoting neurovascular injury (Fig. 9). To verify our hypothesis, we chose to study the bEnd3 cells, a representative in vitro murine BBB model [12,22,32,33], and investigated whether the selective S1PR2 antagonist JTE013 [19,22,38] could protect endothelial barrier integrity during acute focal ischemia using the mouse pMCAO model.

By activation of the Erk1/2 pathway, but not p38 pathway, H_2O_2 influences paracellular permeability of porcine brain-derived microvascular ECs [16]. Erk1/2, activated by MEK1/2, regulates cPLA$_2$ phosphorylation and AA release, which mediates cerebral ischemia-induced oxidative injury [11]. Importantly, both PD98059 [27] and U0126 [39], widely applied to block MEK1/2/Erk1/2 pathway, reduced tMCAO-induced cerebral injury. Our results showed that H_2O_2 in bEnd3 cells induced the phosphorylation of Erk1/2 and cPLA$_2$ with a similar time course. Moreover, we revealed that FR180204, a selective

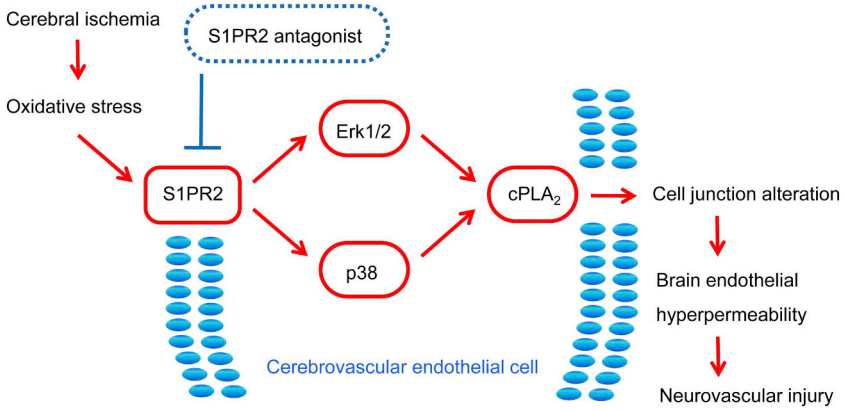

Fig. 9. Schematic diagram of the protective effect of S1PR2 antagonist on endothelial barrier integrity impairment after cerebral ischemia.

Erk1/2 inhibitor [40], inhibited H_2O_2-induced concomitant Erk1/2 and $cPLA_2$ phosphorylation in a dose-dependent manner, like U0126. And it should be noted that neither U0126 nor FR180204 could affect the phosphorylation of p38 in response to H_2O_2, confirming that the Erk1/2 activation is directly required for the $cPLA_2$ phosphorylation in H_2O_2-stimulated brain microvascular ECs. Although H_2O_2 stimulation induced a sustained high level of p38 phosphorylation in vitro, the selective p38 inhibitor SB203580 attenuated $cPLA_2$ phosphorylation, indicating that p38 is also the direct upstream kinase of $cPLA_2$ phosphorylation, which does not depend on Erk1/2. Concurring with these observations, p38 inhibition led to a decrease in H_2O_2-enhanced bEnd3 monolayer permeability, though less robustly than Erk1/2 inhibition. In this regard, the more robust effect of Erk1/2 inhibtion on endothelial permeability change under oxidative stress could be mediated by downstream factors other than $cPLA_2$. Together, our results clearly showed that Erk1/2 and p38 were involved in H_2O_2-enhanced $cPLA_2$ phosphorylation and brain endothelial permeability, respectively.

Interendothelial cell junction proteins modulate paracellular permeability [6,41] and physical properties of BBB [3]. And the loss of TJ and AJ proteins induced by cerebral ischemia enhanced BBB permeability [42]. The transmembrane protein claudin-5, occludin and ZO-1 are essential molecules participating in the formation of BBB structural component TJs [7], while AJs are mainly formed by interactions of VE-cadherin between adjacent cells and required to maintain vascular endothelial integrity [6,41]. Additionally, CD31 which is highly expressed at EC junctions influences barrier stabilization [43]. Our in vitro data demonstrated that H_2O_2 stimulation at a high concentration (2 mM) [44], which did not affect the junction protein expression in bEnd3 cells, increased the permeability to FITC-labeled dextran. Moreover, ZO-1 junctional localization was no longer obvious at the region where ECs were not in contact. These results are consistent with the report that H_2O_2 increases paracellular permeability accompanied with redistribution of ZO-1 [15]. Meanwhile, our data suggested that $cPLA_2$ inhibitor CAY10502 [45] as well as S1PR2 antagonist JTE013 pretreatment partially reversed the changes of paracellular permeability and ZO-1 subcellular localization induced by H_2O_2, indicating that both S1PR2 and $cPLA_2$ could regulate the permeability of cerebrovascular endothelium in response to exogenous oxidative stress. Furthermore, our findings that shS1PR2-infected bEnd3 cells, in the presence of H_2O_2, exhibited a continuous ZO-1 distribution at cell junctions and a dramatic decrease in paracellular hyperpermeability also raise the intriguing possibility that S1PR2 targeting could be beneficial to prevent the development of brain EC barrier impairment under oxidative stress.

Then we found that JTE013 abrogated H_2O_2-evoked phosphorylation of p38, Erk1/2 and $cPLA_2$, and confirmed the involvement of S1PR2 in this process by RNA interference experiments, supporting our hypothesis that S1PR2 regulates H_2O_2-enhanced brain EC permeability via p38-$cPLA_2$ and Erk1/2-$cPLA_2$ pathway. As a highly stable membrane-associated ROS [14], H_2O_2 up-regulates the activity of sphingosine kinase, leading to intracellular S1P generation and its subsequent release in ECs [46]. However, S1P attenuated H_2O_2-induced p38 phosphorylation and caspase-3 activation in vascular ECs [47]. And S1P was protective for chronic intermittent hypoxia-induced endothelial cell injury involving increased intracellular ROS [48]. Because the oxygen and glucose deprivation of 6 h followed by reperfusion of 6 h resulted in upregulation of S1PR2 messenger RNA in bEnd3 cells [22], H_2O_2 simulation of only 30 min or 1 h might not be sufficient to enhance the expression of S1PR2 in our in vitro studies. Thus, we believe that H_2O_2 could directly activate S1PR2 signaling pathway or membrane translocation at the cell surface. Although the bEnd3 cell line is a well-established in vitro model of murine cerebrovascular endothelium [12,22], it is not clear whether other BBB-associated cell types such as astrocytes, pericytes, and neurons might be implicated in ROS activation of endothelial S1PR2 under oxidative stress.

To validate the in vitro observations in vivo, we used the permanent focal cerebral ischemia model. JTE013 administration decreased the cerebrovascular EBD extravasation and reversed the decrease in endothelial junction protein levels in ipsilateral hemispheres after pMCAO, implying that S1PR2 activation impairs BBB integrity through endothelial cell-cell adhesion in ischemic injury. Moreover, blockade of S1PR2 by JTE013 did not inhibit the decrease in the synaptic protein PSD95 expression level after pMCAO, suggesting that S1PR2 is not critical for the direct regulation of neuronal injury in ischemic stroke. Then using the RNA interference, we investigated the direct regulatory role of S1PR2 in ischemic BBB damage. In the ipsilateral cortex of mice, the S1PR2 knockdown attenuated the EBD extravasation after pMCAO, indicating an amelioration of BBB breakdown. However, further investigation with EC-specific gene-deficient mice would be required to confirm the precise role of S1PR2 in regulating cerebrovascular endothelial permeability.

Consistently, our results suggested that JTE013 reduced total brain edema which is the sum of cytotoxic and vasogenic edema in permanent focal cerebral ischemia in mice. We also found it reduced infarction volume and improved neurological outcome, suggesting that S1PR2 antagonist reduces neuronal injury after I/R of tMCAO [22] as well as in the acute phase of pMCAO. The previous studies using tMCAO [10,11,25–27,39] supports our signaling findings in vitro, and p38 activation and $cPLA_2$ expression is related to BBB disruption in pMCAO [49]. Thus, it may be speculated that blockade of S1PR2, through suppression of p38 and Erk1/2-dependent $cPLA_2$ phosphorylation, could decrease cerebral ischemia-enhanced endothelial permeability in vivo.

5. Conclusion

In the present study, we provide evidence that pharmacological blockade and gene knockdown of S1PR2 ameliorated H_2O_2-enhanced endothelial permeability via the attenuation of p38 and Erk1/2-dependent $cPLA_2$ phosphorylation in vitro and brain endothelial barrier impairment in pMCAO in vivo. Our data suggest that S1PR2 regulates oxidative stress-induced endothelial barrier impairment, and S1PR2-MAPK-$cPLA_2$ signaling could be considered as a potential pathway for the treatment of oxidative stress-related ischemic diseases such as stroke.

Supplementary data to this article can be found online at https://doi.org/10.1016/j.cellsig.2018.09.019.

Acknowledgements

This work was supported by the Natural Science foundation of China (No. 81773724 & 81573424).

Author Contributions

SNL and CCC conceived the project and designed the study. CCC, LD, JYM and XFW performed the experiments and analyzed the data. YLH and LJ contributed to lentivirus experiments. CZ contributed to transwell assay experiments. SNL, CCC, LJ and CZ wrote the manuscript and prepared the figures. All authors reviewed the manuscript.

Competing financial interests

The authors declare no competing financial interests.

References

[1] J.M. Simard, T.A. Kent, M. Chen, K.V. Tarasov, V. Gerzanich, Brain oedema in focal ischaemia: molecular pathophysiology and theoretical implications, The Lancet. Neurology 6 (2007) 258–268, https://doi.org/10.1016/S1474-4422(07)70055-8.
[2] G.A. Rosenberg, Neurological diseases in relation to the blood-brain barrier, Journal of Cerebral Blood Flow and Metabolism 32 (2012) 1139–1151, https://doi.org/10.1038/jcbfm.2011.197.
[3] Z. Zhao, A.R. Nelson, C. Betsholtz, B.V. Zlokovic, Establishment and Dysfunction of the Blood-Brain Barrier, Cell 163 (2015) 1064–1078, https://doi.org/10.1016/j.cell.2015.10.067.
[4] B. Obermeier, R. Daneman, R.M. Ransohoff, Development, maintenance and disruption of the blood-brain barrier, Nat. Med. 19 (2013) 1584–1596, https://doi.org/10.1038/nm.3407.
[5] B.W. Chow, C. Gu, The molecular constituents of the blood-brain barrier, Trends Neurosci. 38 (2015) 598–608, https://doi.org/10.1016/j.tins.2015.08.003.
[6] E. Dejana, F. Orsenigo, Endothelial adherens junctions at a glance, J. Cell Sci. 126 (2013) 2545–2549, https://doi.org/10.1242/jcs.124529.
[7] C. Forster, Tight junctions and the modulation of barrier function in disease, Histochem. Cell Biol. 130 (2008) 55–70, https://doi.org/10.1007/s00418-008-0424-9.
[8] P.A. Fraser, The role of free radical generation in increasing cerebrovascular permeability, Free Radic. Biol. Med. 51 (2011) 967–977, https://doi.org/10.1016/j.freeradbiomed.2011.06.003.
[9] O. Peters, et al., Increased formation of reactive oxygen species after permanent and reversible middle cerebral artery occlusion in the rat, Journal of Cerebral Blood Flow and Metabolism 18 (1998) 196–205, https://doi.org/10.1097/00004647-199802000-00011.
[10] C. Nito, et al., Role of the p38 mitogen-activated protein kinase/cytosolic phospholipase A2 signaling pathway in blood-brain barrier disruption after focal cerebral ischemia and reperfusion, Journal of Cerebral Blood Flow and Metabolism 28 (2008) 1686–1696, https://doi.org/10.1038/jcbfm.2008.60.
[11] K. Kishimoto, et al., Cytosolic phospholipase A2 alpha amplifies early cyclooxygenase-2 expression, oxidative stress and MAP kinase phosphorylation after cerebral ischemia in mice, J. Neuroinflammation 7 (2010) 42, https://doi.org/10.1186/1742-2094-7-42.
[12] C. Betzen, et al., Oxidative stress upregulates the NMDA receptor on cerebrovascular endothelium, Free Radic. Biol. Med. 47 (2009) 1212–1220, https://doi.org/10.1016/j.freeradbiomed.2009.07.034.
[13] N. Ardanaz, P.J. Pagano, Hydrogen peroxide as a paracrine vascular mediator: regulation and signaling leading to dysfunction, Exp. Biol. Med. 231 (2006) 237–251.
[14] B.Y. Jin, A.J. Lin, D.E. Golan, T. Michel, MARCKS protein mediates hydrogen peroxide regulation of endothelial permeability, Proc. Natl. Acad. Sci. U. S. A. 109 (2012) 14864–14869, https://doi.org/10.1073/pnas.1204974109.
[15] H.S. Lee, et al., Hydrogen peroxide-induced alterations of tight junction proteins in bovine brain microvascular endothelial cells, Microvasc. Res. 68 (2004) 231–238, https://doi.org/10.1016/j.mvr.2004.07.005.
[16] S. Fischer, M. Wiesnet, D. Renz, W. Schaper, H2O2 induces paracellular permeability of porcine brain-derived microvascular endothelial cells by activation of the p44/42 MAP kinase pathway, Eur. J. Cell Biol. 84 (2005) 687–697, https://doi.org/10.1016/j.ejcb.2005.03.002.
[17] K. Yanagida, et al., Size-selective opening of the blood-brain barrier by targeting endothelial sphingosine 1-phosphate receptor 1, Proc. Natl. Acad. Sci. U. S. A. 114 (2017) 4531–4536, https://doi.org/10.1073/pnas.1618659114.
[18] M.J. Lee, et al., Vascular endothelial cell adherens junction assembly and morphogenesis induced by sphingosine-1-phosphate, Cell 99 (1999) 301–312.
[19] T. Sanchez, et al., Induction of vascular permeability by the sphingosine-1-phosphate receptor-2 (S1P2R) and its downstream effectors ROCK and PTEN, Arteriosclerosis, Thrombosis, and Vascular Biology 27 (2007) 1312–1318, https://doi.org/10.1161/ATVBAHA.107.143735.
[20] A. Vestri, F. Pierucci, A. Frati, L. Monaco, E. Meacci, Sphingosine 1-phosphate receptors: do they have a therapeutic potential in cardiac fibrosis? Front. Pharmacol. 8 (2017) 296, https://doi.org/10.3389/fphar.2017.00296.
[21] R. van Doorn, et al., Sphingosine 1-phosphate receptor 5 mediates the immune quiescence of the human brain endothelial barrier, J. Neuroinflammation 9 (2012) 133, https://doi.org/10.1186/1742-2094-9-133.
[22] G.S. Kim, et al., Critical role of sphingosine-1-phosphate receptor-2 in the disruption of cerebrovascular integrity in experimental stroke, Nat. Commun. 6 (2015) 7893, https://doi.org/10.1038/ncomms8893.
[23] L.L. Lin, et al., cPLA2 is phosphorylated and activated by MAP kinase, Cell 72 (1993) 269–278.
[24] C.C. Leslie, Properties and regulation of cytosolic phospholipase A2, J. Biol. Chem. 272 (1997) 16709–16712.
[25] J.V. Bonventre, et al., Reduced fertility and postischaemic brain injury in mice deficient in cytosolic phospholipase A2, Nature 390 (1997) 622–625, https://doi.org/10.1038/37635.
[26] J. Zhang, N. Barasch, R.C. Li, A. Sapirstein, Inhibition of cytosolic phospholipase a (2) alpha protects against focal ischemic brain damage in mice, Brain Res. 1471 (2012) 129–137, https://doi.org/10.1016/j.brainres.2012.06.031.
[27] A. Alessandrini, S. Namura, M.A. Moskowitz, J.V. Bonventre, MEK1 protein kinase inhibition protects against damage resulting from focal cerebral ischemia, Proc. Natl. Acad. Sci. U. S. A. 96 (1999) 12866–12869.
[28] L.Y. Chen, G. Woszczek, S. Nagineni, C. Logun, J.H. Shelhamer, Cytosolic phospholipase A2alpha activation induced by S1P is mediated by the S1P3 receptor in lung epithelial cells, American Journal of Physiology. Lung cellular and molecular physiology 295 (2008) L326–L335, https://doi.org/10.1152/ajplung.00393.2007.
[29] C. Zhu, C. Cao, L. Dai, J. Yuan, S. Li, Corticotrophin-releasing factor participates in S1PR3-dependent cPLA2 expression and cell motility in vascular smooth muscle cells, Vasc. Pharmacol. 71 (2015) 116–126, https://doi.org/10.1016/j.vph.2015.03.013.
[30] J.E. Jung, et al., Reperfusion and neurovascular dysfunction in stroke: from basic mechanisms to potential strategies for neuroprotection, Mol. Neurobiol. 41 (2010) 172–179, https://doi.org/10.1007/s12035-010-8102-z.
[31] E. Juttler, M. Kohrmann, P.D. Schellinger, Therapy for early reperfusion after stroke, Nature Clinical Practice. Cardiovascular Medicine 3 (2006) 656–663, https://doi.org/10.1038/ncpcardio0721.
[32] J.A. Shin, J.C. Yoon, M. Kim, E.M. Park, Activation of classical estrogen receptor subtypes reduces tight junction disruption of brain endothelial cells under ischemia/reperfusion injury, Free Radic. Biol. Med. 92 (2016) 78–89, https://doi.org/10.1016/j.freeradbiomed.2016.01.010.
[33] H. Qosa, et al., Differences in amyloid-beta clearance across mouse and human blood-brain barrier models: kinetic analysis and mechanistic modeling, Neuropharmacology 79 (2014) 668–678, https://doi.org/10.1016/j.neuropharm.2014.01.023.
[34] Z. Huang, et al., Effects of cerebral ischemia in mice deficient in neuronal nitric oxide synthase, Science 265 (1994) 1883–1885.
[35] L. Zhou, et al., Treatment of cerebral ischemia by disrupting ischemia-induced interaction of nNOS with PSD-95, Nat. Med. 16 (2010) 1439–1443, https://doi.org/10.1038/nm.2245.
[36] J.C. Jimenez, et al., Anxiety Cells in a Hippocampal-Hypothalamic Circuit, Neuron 97 (2018), https://doi.org/10.1016/j.neuron.2018.01.016 670-683 e676.
[37] M. Asahi, et al., Effects of matrix metalloproteinase-9 gene knock-out on the proteolysis of blood-brain barrier and white matter components after cerebral ischemia, J. Neurosci. 21 (2001) 7724–7732.
[38] S. Del Galdo, C. Vettel, D.M. Heringdorf, T. Wieland, The activation of RhoC in vascular endothelial cells is required for the S1P receptor type 2-induced inhibition of angiogenesis, Cell. Signal. 25 (2013) 2478–2484, https://doi.org/10.1016/j.cellsig.2013.08.017.
[39] M. Henriksson, E. Stenman, P. Vikman, L. Edvinsson, MEK1/2 inhibition attenuates vascular ETA and ETB receptor alterations after cerebral ischaemia, Exp. Brain Res. 178 (2007) 470–476, https://doi.org/10.1007/s00221-006-0753-7.
[40] T. Anastassiadis, et al., A highly selective dual insulin receptor (IR)/insulin-like growth factor 1 receptor (IGF-1R) inhibitor derived from an extracellular signal-regulated kinase (ERK) inhibitor, J. Biol. Chem. 288 (2013) 28068–28077, https://doi.org/10.1074/jbc.M113.505032.
[41] A. Benn, C. Bredow, I. Casanova, S. Vukicevic, P. Knaus, VE-cadherin facilitates BMP-induced endothelial cell permeability and signaling, J. Cell Sci. 129 (2016) 206–218, https://doi.org/10.1242/jcs.179960.
[42] C. Bouleti, et al., Protective effects of angiopoietin-like 4 on cerebrovascular and

functional damages in ischaemic stroke, Eur. Heart J. 34 (2013) 3657–3668, https://doi.org/10.1093/eurheartj/eht153.
[43] J.R. Privratsky, P.J. Newman, PECAM-1: regulator of endothelial junctional integrity, Cell Tissue Res. 355 (2014) 607–619, https://doi.org/10.1007/s00441-013-1779-3.
[44] K. Takeuchi, et al., AMP-dependent kinase inhibits oxidative stress-induced caveolin-1 phosphorylation and endocytosis by suppressing the dissociation between c-Abl and Prdx1 proteins in endothelial cells, J. Biol. Chem. 288 (2013) 20581–20591, https://doi.org/10.1074/jbc.M113.460832.
[45] J.M. Barnett, G.W. McCollum, J.S. Penn, Role of cytosolic phospholipase a(2) in retinal neovascularization, Invest. Ophthalmol. Vis. Sci. 51 (2010) 1136–1142, https://doi.org/10.1167/iovs.09-3691.
[46] P. Xia, et al., Tumor necrosis factor-alpha induces adhesion molecule expression through the sphingosine kinase pathway, Proc. Natl. Acad. Sci. U. S. A. 95 (1998) 14196–14201.
[47] T. Moriue, et al., Sphingosine 1-phosphate attenuates H2O2-induced apoptosis in endothelial cells, Biochem. Biophys. Res. Commun. 368 (2008) 852–857, https://doi.org/10.1016/j.bbrc.2008.01.155.
[48] F.C. Yu, et al., Protective effect of sphingosine-1-phosphate for chronic intermittent hypoxia-induced endothelial cell injury, Biochem. Biophys. Res. Commun. 498 (2018) 1016–1021, https://doi.org/10.1016/j.bbrc.2018.03.106.
[49] L. Cui, et al., Neuroprotection of early and short-time applying atorvastatin in the acute phase of cerebral ischemia: down-regulated 12/15-LOX, p38MAPK and cPLA2 expression, ameliorated BBB permeability, Brain Res. 1325 (2010) 164–173, https://doi.org/10.1016/j.brainres.2010.02.036.